A HIGH-ENERGY PULSED-POWER SUPPLY, SUITABLE FOR HIGH-POWER MICROWAVE SOURCES

P. MacInnes, I. V. Konoplev, A. W. Cross, C. G. Whyte, W. He, H. Yin, C. W. Robertson, A. R. Young, A. D. R. Phelps and K. Ronald

SUPA Department of Physics, University of Strathclyde, Glasgow
Lanarkshire, G4 0NG, Scotland

Abstract

This paper presents a, high-energy, pulsed-power-supply, developed at the University of Strathclyde for use in high-energy microwave source research. The supply was based on a, reconfigurable, inverting Marx generator, coupled to a folded transmission-line pulse former.

The present configuration offers nominally 200ns long pulses, with amplitudes of up to 1MV and beam currents on the order of 100kA (i.e. ~20kJ, limited by the Marx generator). Reconfigured with a higher capacity Marx-bank, allows operation of the pulse former at its full output power rating of 0.2TW for 200ns (1MV, 200kA, into a matched load, providing 40kJ).

I. INTRODUCTION

One of the on-going research projects, at the University of Strathclyde, is the development of a high-power, 8mm wavelength, Free-Electron Maser (FEM). The FEM exploits the novel dispersive characteristics offered by Bragg reflectors [1-8] to define the microwave lasing cavity, operating as a highly mode selective, single-frequency oscillator [9-13]. Such FEM's require highly mono-energetic, mildly relativistic (0.4 – 1MeV), electron beams, with beam currents of a few kilo-amperes and pulse durations on the order of a few hundred nanoseconds.

To deliver such pulses a magnetically insulated, space-charge-limited, accelerating diode was developed, driven by a high-energy pulsed-power-supply (PPS) [13].

II. THE HIGH-ENERGY PULSED POWER SUPPLY

The specification for the PPS was derived largely from the anticipated requirements of the accelerating diode, i.e. it had to provide well defined "rectangular" pulses of ~200ns at amplitudes of 0.4-1MV and driving currents ranging from 1-10kA. However, given the nature of the space-charge limited diode, the estimated maximum current requirement was increased by an order of magnitude; such accelerating diodes employ explosive emission cathodes, which generate plasma close to the cathode surface, which then expands towards the anode, giving a diode perveance which evolves over the duration of the pulse. This affects the load impedance; as the cathode plasma expands, the load impedance typically decreases, necessitating an increase in the driving current if the applied potential is to be maintained. The maximum current available from the supply must therefore be sufficient to ensure the accelerating gradient on the beam electrons is not adversely affected.

With the previously mentioned requirements in mind, the base performance for the PPS was determined to be:

Table 1. Base Specification for the PPS.

Parameter	Value / Units
Pulse amplitude	0.4 – 1MV
Pulse duration	200 – 250ns
Pulse shape	Rectangular
Available current	100 – 200kA

To achieve this, a two-stage pulse generator was developed, with the initial stage consisting of a high-voltage (in excess of 1MV) Marx-generator and the final stage consisting of a pulse-forming transmission line.

A. The Marx-Generator

The Marx-generator was designed to allow relative ease in reconfiguration, with the construction based around a simple capacitor stack, allowing for the removal or addition of stages, either placed in series or in parallel. A cross-section of the current configuration is presented in Fig. 1.

The generator was configured as an "inverting-Marx", i.e. the capacitor stack was charged under a positive potential, to provide a negative output potential. The charging supply was a Glassman PK100R040 DC supply (maximum output +/- 100kV, 40mA), typically operated in the range 40-55kV, 3-8mA. The Marx capacitors were charged in parallel, with breakdown prevented via a dry-nitrogen spark-gap (SG) column, maintained under a positive pressure (i.e. to the right of the Paschen minimum). The pressure in the column was adjustable to within ±0.5PSI using a precision pressure regulator. The initial SG incorporated a mid-plane electrode in the intra-electrode spacing, maintained at a floating positive potential ~$0.25V_0$ during the charging cycle (where V_0 is the charging voltage from the DC supply).

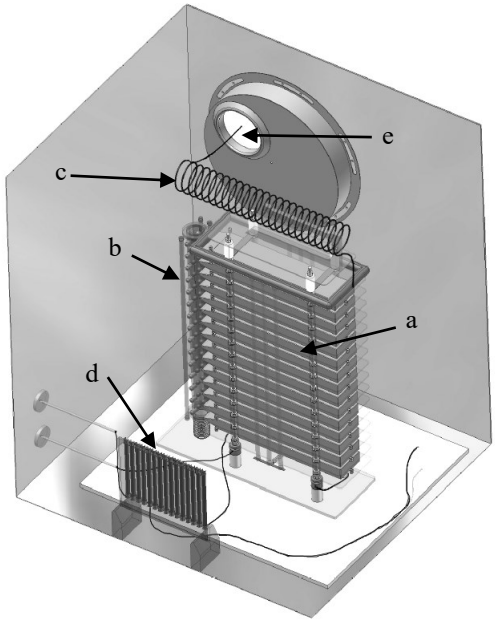

Figure 1. The Marx-generator. (a) Capacitor stack, (b) Spark-gap column, (c) Inductor coil, (d) Charging resistors, (e) Connection to pin "b" (see Fig. 4)

Once fully charged the Marx capacitors could then be actively discharged via a thyratron switch; on triggering of the thyratron, the potential of the mid-plane electrode was pulled to ground, initiating break-down of the first SG, over-volting the second and so on. The Marx therefore erects in series, giving a maximum output voltage proportional to the nV_0, where n is the number of stages in the Marx-stack. The closing SGs generated bursts of UV light, providing a degree of "priming" to the subsequent gaps, enhancing the erection time.

The Marx configuration presented in Fig. 1 (and in the following results) consisted of a stack of 15 General Atomic 100kV, 0.3μF capacitors, giving a maximum output voltage of 1.5MV at a maximum discharge current of 25kA. The maximum energy storage was 22.5kJ (an alternative configuration would be employed to drive the PPS to higher energy levels). Excluding the charging supply and thyratron, the apparatus discussed above was located within an oil-filled isolation tank, to prevent breakdown under load.

The discharge from the Marx-generator was monitored using a resistive divider probe; an example of the measured pulse profile is presented in Fig. 2. The discharge curve shown in Fig. 2 represents a charging voltage on the Marx capacitors of ~53kV, giving a peak output voltage of ~0.8MV. The pulse shape is indicative of the CLC circuit presented by the Marx, its capacitive load and the inductance of the coil connecting the two (Fig. 1(c)). The inductor coil allows for resonant coupling of the two effective capacitances (that of the Marx and its load) and prevents the Marx discharge current from exceeding the maximum rating of 25kA.

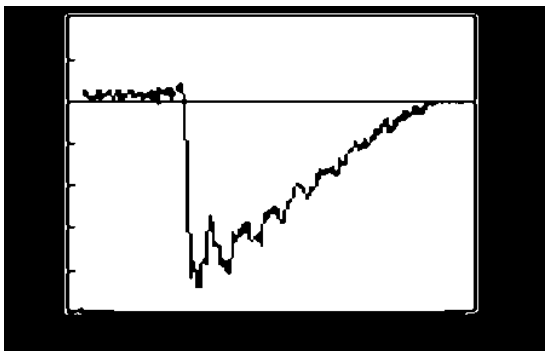

Figure 2. Typical discharge curve from the Marx-generator.

The capacitive "load" of the Marx-generator was a passively switched, spark-gap terminated, pulse forming line. The design is presented in Section B.

B. The Pulse Forming Line

In order to obtain the required "rectangular" pulse profile from the PPS, the output of the Marx-generator was coupled into a "folded" transmission line. A basic schematic of which is given in Fig. 3.

Figure 3. Basic circuit schematic of the folded transmission line.

The folded line functions in much the same manner as a standard transmission line; the incident voltage from the Marx (V_{Marx}) charges the line. Once charged, the line is discharged by closing the output switch (in this case a passively switched SG), allowing the line to discharge to an attached load. If the effective impedance, presented by the matching resistors (R_1) and the load (R_L), is properly matched to the impedance of the line, this gives the desired "rectangular" pulse shape, with a peak amplitude of $V_{Marx}/2$ and a pulse duration determined by the physical length of the line and its dielectric filling (i.e. by its electrical length). Electrically the folded line differs in this respect, from the standard line, in that a given physical length provides twice the electrical length when compared to the standard line. For the PPS presented here, the SG noted in Fig. 3 was positioned in a second oil-filled isolation tank, with connection to the transmission line afforded by HT cabling as described below.

1) The Folded Transmission Line

To provide the required voltage hold-off, of up-to 1MV, the pulse forming line was constructed using a set

of large diameter stainless-steel tubes, the outer most of which had a mean diameter of 70cm and a total length of 2m. The physical geometry is shown in cross-section in Fig. 4. A ratio of 2:1 was used between successive conductor radii.

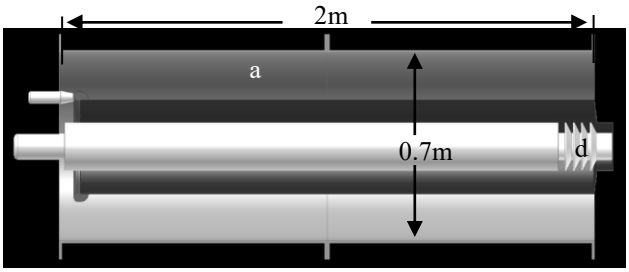

Figure 4. The geometry of the folded transmission line in cross-section. (a) grounded outer conductor, (b) HT connection of mid-conductor, (c) GND connection pin of centre conductor, (d) dielectric support

Corrugated polypropylene plates were used to terminate the ends of the line. This prevented ingress of oil, which would affect the line dielectric, and provided support to (and insulation of) the intermediate conductors. The choice of insulator material used at this point was important, as deionised water quickly degrades nylon whereas Perspex (while resistant to the ionizing effects of the water) does not possess the elasticity required to absorb the shock-wave produced if the HT spark-gap were to misfire.

Looking at Fig. 4, the outer conductor was grounded via a bolted connection to the Marx and output-SG isolation tanks. The mid-conductor was connected to the output coil of the Marx using a large radius pin (Fig. 4(b)), which was attached to the mid-conductor via a field-relieving annulus. The mid-conductor was supported, at the charging side, by the intrusion of the pin through the polypropylene insulation plate. Similarly, the "fold" in the mid-conductor was supported by the polypropylene plate at the discharge side (this can be seen in Fig. 5(b)). The centre conductor was supported, at the charging side, both by its grounded pin connection to the Marx insulation tank (Fig. 4(c)) and by the polypropylene plate. Support was offered at the discharge side via a piece of corrugated polypropylene, attached to the inner surface of the "fold" in the mid-conductor. The corrugation increases the tracking distance between the two conductors, aiding in suppression of electrical breakdown.

The deionised water of the line was maintained at a resistivity of ~17MΩcm by a pair of Barnstead EPure deionizers, run in parallel by a diaphragm pump operating at 4-5Bar. The input and output, to and from, the deionizer circuit was taken from a lower pressure, high flow, circulating loop, driven by a stainless steel, 60ltr/min Lowara centrifugal pump. This ensured sufficient flow from the transmission line, to the deionizer circuit, to maintain the resistivity, whilst also minimizing turbulence in the line; turbulence generates non-linear changes in the effective dielectric constant, reducing the performance of the pulse former.

2) The High-Tension Spark-Gap

The HT SG, located at the output of the transmission-line, can be seen in Fig. 5.

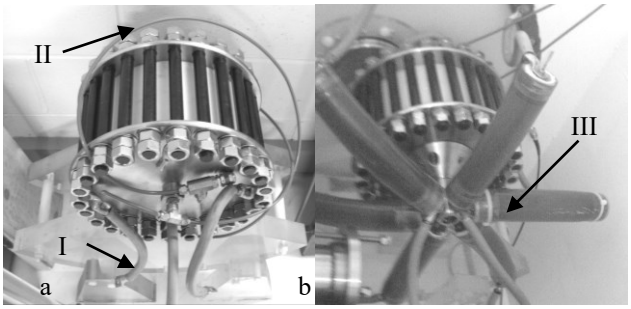

Figure 5. (a) HT SG, showing (I) connection cables to the mid-conductor, (II) dry-nitrogen gas line, (b) HT SG in position, showing (III) matching resistors (R_1).

The pressure vessel of the SG was formed using a ~7cm walled, 15cm long nylon tube, with an ID of ~12cm, sealed using two 1cm thick stainless steel plates held tight by a series of 24 high-strength, glass-reinforced, M22, shanked, nylon rods. This allowed the SG to be pressurized, using dry-nitrogen, up to a (tested) limit of 20Bar, though this is not necessarily indicative of the maximum operating pressure. Pressure control was offered to within ±5PSI using a 0-20Bar, self-relieving, regulator.

Brass electrodes were attached, internally, to the steel plates, with the HT electrode incorporating the gas feed into the pressure vessel (see Fig. 5(a)). The matching resistors (R_1 from Fig. 3) were connected to the GND electrode (see Fig. 5(b)) and placed in parallel with the connection to the accelerating diode (R_L from Fig. 3).

To monitor the profile of the output pulse, a high-voltage, resistive-divider probe was connected across the output of the line. A comparison of 8 shots, taken for a charging voltage on the Marx of 50kV, is given in Fig. 6. This provided nominally 200ns long pulses at a mean amplitude of ~500kV.

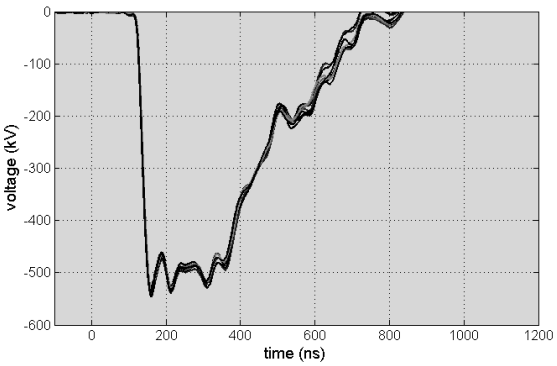

Figure 6. Comparison overlay of 8 shots from the PPS, for a charging voltage of 50kV on the Marx capacitors.

It should be noted that the deviation observed, across the peak of the pulses, is indicative of capacitive ringing due to stray-capacitance in the diagnostic, not the actual uniformity of the pulse shape. This is explained further in Section III. The stepped decay, observed, was the result of a deliberate mismatch between the effective load and line impedances; the load impedance was set higher than the line impedance, to deliver closer to $0.65V_{Marx}$ at the output of the line, consistent with the voltage profile shown in Fig. 6.

This configuration decreases the maximum available energy in the "useful" portion of the pulse, however this was still far in excess of that required by the microwave sources under investigation (0.1 – 1kJ), so had minimal impact. We could therefore exploit the impedance mismatch to minimize the electrical stresses imposed on the Marx capacitors for a given operating voltage.

Should a more uniform pulse shape be required, a proper match between the load and line impedances can be obtained, either through the use of a low impedance diode (with R_1 removed), or more typically by increasing the concentration of $CuSO_4$ in the matching resistors. An example of a pulse taken under the latter condition is given in Fig. 7.

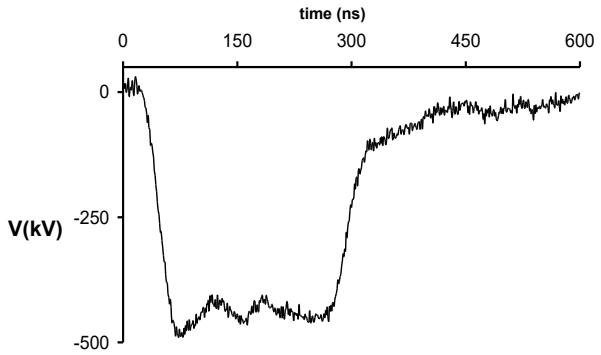

Figure 7. Pulse profile from the PPS operating into a near matched effective load impedance.

The PPS can therefore have its output-pulse profile tuned relatively simply, allowing it to account for different diode configurations (and so impedances) and different operating regimes as required. With the current Marx-generator configuration, operating with the line output set at $\sim 0.65V_{Marx}$, this allows for a maximum voltage output of ~1MV from the line, driving a total current in the region of 100kA, for ~200ns (~20kJ in the pulse from the PPS). For a matched load, operating at 1MV, a change in Marx-generator configuration would be required, however, taking the line impedance as being nominally 5Ω, such a change would allow for a maximum current limit of 200kA, delivering 1MV for the 200ns duration of the pulse, corresponding to an upper energy limit of 40kJ.

III. FREE-ELECTRON MASERS DRIVEN BY THE PULSED POWER SUPPLY

The PPS configuration presented (utilizing the 15-stage Marx-generator) was used to drive the accelerating diode in a series of high-power FEM single-frequency oscillators [11-13] based on Bragg Reflector cavities. A cross-section of the diode is given in Fig. 8.

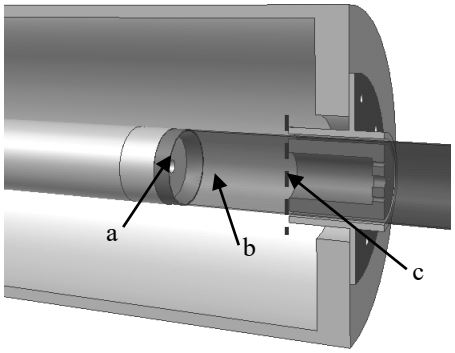

Figure 8. (a) annular cathode emitter, (b) high-current annular electron beam, (c) entrance to coaxial drift-tube (anode-plane).

Electron beams of ~0.5MeV, 1-4kA were transported, under magnetic insulation of ~0.6-0.8T, through a coaxial drift-tube, incorporating the FEM lasing cavity (See Fig. 9), with lasing induced using a azimuthally symmetric, periodic magnetic-field.

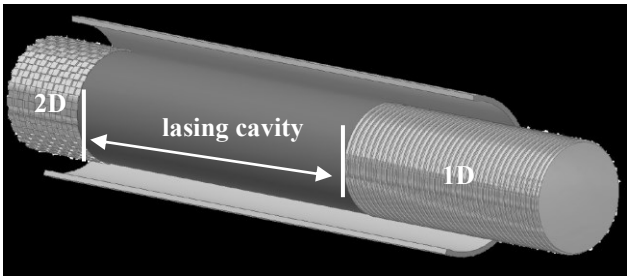

Figure 9. A coaxial drift-tube, incorporating a lasing cavity provided by 2D – 1D Bragg reflectors on the inner conductor

This generated microwave pulses with durations on the order of ~150ns, at integrated output-power levels of 60MW(+/- 10%). The Fourier content of the pulses was evaluated as being strongly peaked at a single frequency of ~37.3GHz (see Fig. 10).

The strongly mono-chromatic output from the FEM provides additional confirmation of the successful operation of the PPS, as the FEM resonant frequency depends directly on the accelerating potential; if the variation seen in the peak of the applied voltage pulse, as measured by the resistive divider probe, was physical, the resultant variation in the electron energies would produce

a broadening of the spectral content, limited by the band-width of the lasing cavity resonance.

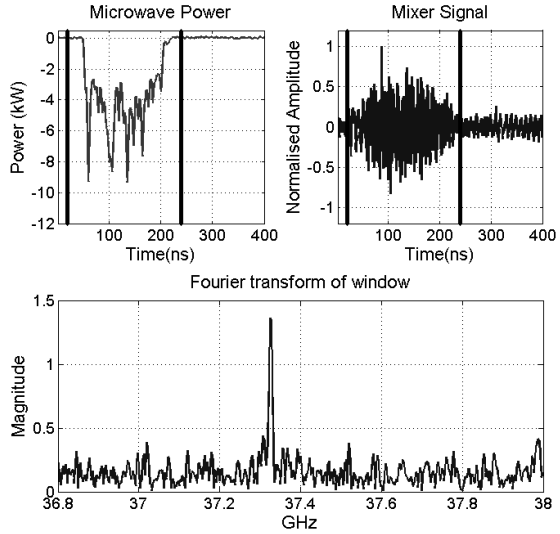

Figure 10. Example pulse from the 2D-1D Bragg FEM experiment, showing the pulse envelope (non-integrated power), pulse waveform and spectral content.

Such behaviour was not observed over the course of multiple experimental runs, utilizing various configurations of both diode and FEM interaction region. This gives a strong indication that the PPS delivers a well defined, "rectangular" accelerating pulse as designed.

IV. SUMMARY

A high-energy pulsed-power-supply has been designed, constructed and successfully tested at the University of Strathclyde. The supply is capable of delivering up to 1MV for ~200ns at its output, either into an unmatched load, using the current Marx-generator, or into a matched load with the Marx reconfigured to a higher capacitance. Under its current configuration, the PPS can deliver a maximum of ~20kJ to an attached load, though the pulse former itself is rated to a maximum of 40kJ, for a 1MV pulse into a matched load.

The performance of the supply has been verified both directly, via measurement of the output pulse, and indirectly, via detailed analysis of the measured output from a series of high-power, single-frequency, FEM microwave oscillators.

V. ACKNOWLEDGEMENTS

This work was carried out as part of a UK MoD Research Programme. Support by the UK EPSRC is also gratefully acknowledged.

VI. REFERENCES

[1] H. Kogelnik, C. V. Shank, "Coupled-Wave Theory of Distributed Feedback Lasers", *J. Appl. Phys*., vol. 43(5), pp. 2327-2335, May 1972.

[2] G. G. Denisov, M. G. Resnikov, "Corrugated Cylindrical Resonators for Short-Wavelength Relativistic Microwave Oscillators," *Radio Physics and Quantum Electronics*, vol. 25(5), pp. 407-413, 1982.

[3] A. W. Cross, W. He, I. V. Konoplev, A. D. R. Phelps, K. Ronald, G. R. M. Robb, C. G. Whyte, N. S. Ginzburg, N. Yu. Peskov, A. S. Sergeev, "Experimental and theoretical Study of 2D Bragg structures for a coaxial free electron maser", *Nuclear Instruments and Methods in Physics Research A*, vol. 475, pp. 164 – 172, December 2001.

[4] N. S. Ginzburg, N. Yu. Peskov, A. S. Sergeev, I. V. Konoplev, A. W. Cross, A. D. R. Phelps, G. R. M. Robb, K. Ronald, W. He, C. G. Whyte, "Theory of free-electron maser with two-dimensional distributed feedback driven by an annular electron beam", *J. Appl. Phys*., vol. 92(3), pp.1619-1629, August 2002.

[5] A. W. Cross, I. V. Konoplev, A. D. R. Phelps, K. Ronald, "Studies of surface two-dimensional photonic band-gap structures", *J. Appl. Phys*., vol. 93(4), pp. 2208 – 2218, February 2003.

[6] M. I. Fuks, M. B. Goikhman, N. F. Kovalev, A. V. Palitsin, E. Schamiloglu, "Waveguide Resonators with Combined Bragg Reflectors", *IEEE Trans. on Plasma Sci.*, vol. 32(3), pp.1323-1333, June 2004.

[7] N. S. Ginzburg, N. Yu. Peskov, A. S. Sergeev, I. V. Konoplev, K. Ronald, A. D. R. Phelps, A. W. Cross, "On the mechanism of high selectivity of two-dimensional coaxial Bragg resonators", *Nuclear Instruments and Methods in Physics Research A*, vol. 528, pp.78-82, 2004.

[8] I. V. Konoplev, P. McGrane, A. W. Cross, K. Ronald, A. D. R. Phelps, "Wave interference and band gap control in multiconductor one-dimensional Bragg structures", *J. Appl. Phys*., vol. 97(7), article: 073101, 2005.

[9] N. S. Ginzburg, N. Yu. Peskov, A. S. Sergeev, A. D. R. Phelps, A. W. Cross, I. V. Konoplev, "The use of a hybrid resonator consisting of one-dimensional and two-dimensional Bragg reflectors for generation of spatially coherent radiation in a coaxial free-electron laser", *Phys. Plasmas*, vol. 9(6), pp. 2798-2802, June 2002.

[10] I. V. Konoplev, P. McGrane, W. He, A. W. Cross, A. D. R. Phelps, C. G. Whyte, K. Ronald, C. W. Robertson,

"Experimental Study of Coaxial Free-Electron Maser Based on Two-Dimensional Distributed Feedback", *Phys. Rev. Lett.*, vol. 96(3), article: 035002, January 2006

[11] I. V. Konoplev, A. W. Cross, A. D. R. Phelps, W. He, K. Ronald, C. G. Whyte, C. W. Robertson, P. MacInnes, N. S. Ginzburg, N. Yu. Peskov, A. S. Sergeev, V. Yu. Zaslavsky, "Experimental and theoretical studies of coaxial free-electron maser based on two-dimensional distributed feedback", *Phys. Rev. E*, vol. 76(5), article: 056406, 2007.

[12] I. V. Konoplev, P. MacInnes, A. W. Cross, L. Fisher, A. D. R. Phelps, W. He, K. Ronald, C. G. Whyte, C. W. Robertson, "High-Current Electron Beams for High-Power Free-Electron Maser Based on Two-Dimensional Periodic Lattices", *IEEE Trans. Plasma Sci*., vol. 38(4), pp. 751-763, April 2010.

[13] I. V. Konoplev, A. W. Cross, P. MacInnes, W. He, C. G. Whyte, A. D. R. Phelps, C. W. Robertson, K. Ronald, A. R. Young, "High-current oversized annular electron beam formation for high-power microwave research", *Appl. Phys. Lett*., vol. 89(17), article: 171503, 2006.